Research Square

Preprints are preliminary reports that have not undergone peer review.
They should not be considered conclusive, used to inform clinical practice,
or referenced by the media as validated information.

A Combined Life Cycle Assessment and Multi-Scenario Photovoltaic Modelling Framework for Assessing Building Decarbonization in Nusantara

Rudi Chandra Adinugraha
University of Melbourne
Mohammed Ali Berawi
University of Indonesia
Titi Sari Nurul Rachmawati
University of Indonesia
Behzad Rismanchi
brismanchi@unimelb.edu.au
University of Melbourne

Research Article

Keywords: Life cycle assessment, Building-integrated photovoltaics, Decarbonization, High-rise building, Nusantara

Posted Date: November 25th, 2026

DOI: https://doi.org/10.21203/rs.3.rs-11228315/v1

License: This work is licensed under a Creative Commons Attribution 4.0 International License.
Read Full License

Additional Declarations: No competing interests reported.

A Combined Life Cycle Assessment and Multi-Scenario Photovoltaic Modelling Framework for Assessing Building Decarbonization in Nusantara

Rudi Chandra Adinugraha[1,3], Mohammed Ali Berawi[3,4], Titi Sari Nurul Rachmawati[3], and Behzad Rismanchi[1,2,*]

[1] Department of Infrastructure Engineering, The University of Melbourne, Australia
[2] Renewable Energy and Energy Efficiency Group, The University of Melbourne, Australia
[3]Department of Civil and Environmental Engineering, Universitas Indonesia, Indonesia
[4]Center for Sustainable Infrastructure Development (CSID), Universitas Indonesia, Indonesia

*Author to whom any correspondence should be addressed.

E-mail: brismanchi@unimelb.edu.au

Abstract

Indonesia's new capital, Nusantara, aims for net-zero emissions (NZE) by 2045, placing stringent decarbonization pressures on high-density residential developments. In tropical climates, operational cooling has historically dominated building emissions; however, modern energy-efficient designs and aggressive decarbonization timelines necessitate a re-evaluation of whole-life carbon impacts. This study introduces an integrated BIM-LCA-GSA framework to conduct a 20-year cradle-to-grave Life Cycle Assessment (LCA) of a newly constructed 12-storey residential building in Nusantara. The baseline results reveal total emissions of 1.73×10^7 kg CO_2e, demonstrating that Embodied Carbon (EC) from building materials (50.4%) has surpassed Operational Carbon (OC) (49.6%) as the primary emission hotspot over the 20-year horizon. To mitigate these impacts, two façade-integrated Building-Integrated Photovoltaic (BIPV) scenarios were modeled. The optimal 93.0 kWp BIPV system successfully reduced overall building emissions by 10.5% and achieved a financial payback period of 16.3 years, proving its techno-economic viability without feed-in tariffs. Furthermore, variance-based Global Sensitivity Analysis (GSA) confirmed that operational electricity and structural material manufacturing govern the vast majority of output variance. The findings underscore that achieving NZE requires robust policies mandating both operational efficiency and structural material decarbonization.

Keywords: Life cycle assessment, Building-integrated photovoltaics, Decarbonization, High-rise building, Nusantara

---

Abbreviations List

- **BIM**: Building Information Modelling
- **BIPV**: Building-Integrated Photovoltaic
- **EC**: Embodied Carbon
- **EOL**: End-of-Life
- **EPBT**: Energy Payback Time
- **EPD**: Environmental Product Declaration
- **GFA**: Gross Floor Area
- **GHG**: Greenhouse Gas
- **GSA**: Global Sensitivity Analysis
- **GWP**: Global Warming Potential
- **HVAC**: Heating, Ventilation, and Air Conditioning
- **IKN**: Ibu Kota Nusantara
- **LCA**: Life Cycle Assessment
- **LCC**: Life Cycle Costing
- **LCI**: Life Cycle Inventory
- **LCIA**: Life Cycle Impact Assessment
- **NPV**: Net Present Value
- **NZE**: Net-Zero Emissions
- **OAT**: One-at-a-Time
- **OC**: Operational Carbon
- **PP**: Payback Period
- **PR**: Performance Ratio
- **PV**: Photovoltaic
- **QTO**: Quantity Take-Off
- **TMY**: Typical Meteorological Year

Introduction

The built environment accounts for approximately 36% to 40% of global energy consumption and nearly 40% of energy-related carbon dioxide (CO_2) emissions, establishing the construction sector as a central battleground for climate change mitigation and resource conservation [1–3] . Under the Paris Agreement, international frameworks and national decarbonization roadmaps increasingly compel municipalities and urban centers to establish ambitious net-zero emissions (NZE) milestones [4, 5] . In developing economies across Southeast Asia, rapid economic growth and urbanization intensify this environmental challenge [2, 6]. Indonesia, as the world's fourth most populous nation, is currently executing an unprecedented capital city transition from Jakarta to the new smart and sustainable forest capital, Ibu Kota Nusantara (IKN), situated in East Kalimantan [6]. Positioned as a flagship green metropolis, IKN has committed to achieving an economy-wide NZE target by 2045, placing it among the most ambitious administrative capitals globally [6]. As shown in Table 1, Nusantara's 2045 target is highly progressive when compared to the 2050 milestones set by established cities such as Tokyo and Paris [7]. However, realizing carbon neutrality in a newly constructed tropical administrative hub presents profound engineering and environmental trade-offs, particularly regarding the materials selected for high-rise infrastructure versus long-term operational performance [8, 9].

Table 1. Comparison of NZE Target across Different Capital Cities in APAC and Europe

Capital City	NZE Target Year	Main Strategies to Achieve NZE	Source
Nusantara (Indonesia)	2045	100% renewable energy, 65% green/forest area, smart city technologies.	[7]
Canberra (Australia)	2045 (citywide), 2040 (govt ops)	100% renewable electricity, electrification, green transport.	[5]
Tokyo (Japan)	2050	Renewable energy, energy efficiency, green buildings, public transport.	[4]
Paris (France)	2050	Energy retrofits, renewables, sustainable mobility, green spaces.	[4]

Historically, sustainable building initiatives and green building rating systems in the tropics focused almost exclusively on minimizing operational energy demand and operational carbon (OC) emissions through high-efficiency heating, ventilation, and air conditioning (HVAC) systems, low-emissivity glazing, and energy-efficient lighting [2, 10]. While operational efficiency remains critical in equatorial regions characterized by year-round high temperatures and relative humidity [2, 11], aggressive operational decarbonization has precipitated a fundamental paradigm shift across the whole life cycle of buildings [12]. As operating energy intensity decreases and national electrical grids gradually integrate renewable sources [6], embodied carbon (EC) – which encompasses the greenhouse gas (GHG) emissions generated during raw material extraction, manufacturing, transportation, on-site construction, maintenance, refurbishment, and end-of-life (EOL) processing – becomes the dominant contributor to life-cycle global warming potential (GWP) [9, 13]. Table 2 illustrates this shift, demonstrating that while tropical buildings traditionally report OC shares ranging from 74.9% to 90%, newer energy-efficient constructions in temperate regions are already seeing EC shares climb to 66–71% [14, 15].

Table 2. Comparison of embodied and operational carbon shares across building types, climates, and assessment periods

Building Type	Location/Climate	Construction Era	Carbon Proportion (%)		Assessment Period	Source
			Embodied	Operational		
High-rise Office (30-storey)	Malaysia (Tropical)	2020s	25.1%	74.9%	30 years	[14]
High-rise Office (LEED)	Malaysia (Tropical)	2020s	13.4%	86.6%	30 years	[14]
University Buildings	Singapore (Tropical)	2010s	10%	90%	40 years	[16]
High-rise Residential	India (Humid subtropical)	2020s	40%	60%	50 years	[17]
(Pre-1991)	Victoria, Australia (Temperate)	Pre-1991	9-35%	65-91%	Service life	[15]
Residential (1992-2006)	Victoria, Australia (Temperate)	1992-2006	40-55%	45-60%	Service life	[15]
Residential (Post-2011)	Victoria, Australia (Temperate)	2012-2019	66-71%	29-34%	Service life	[15]
Office Building	Europe (Temperate)	2010s	58%	42%	50 years	[18]
Mixed Urban (Metropolitan)	Melbourne, Australia (Temperate)	Mixed	100%*	-	Initial only	[19]
University Buildings	Florida, USA	2000s	81%	19%	50 years	[20]

*Note: *Rydlewski et al. (2022) focused only on embodied carbon assessment. Shading indicates relatively high proportions: red for embodied carbon >40%, blue for operational carbon >60%.*

Because upfront embodied emissions are released into the atmosphere prior to building occupancy, they create an immediate, irreversible "carbon spike" that cannot be mitigated by subsequent operational energy savings [8, 21]. In high-rise institutional buildings, structural systems composed of reinforced concrete and structural steel constitute up to 70% to 90% of total upfront EC [8, 13]. Consequently, evaluating urban developments solely through operational benchmarks introduces substantial carbon blind spots, undermining broader municipal net-zero commitments [4, 12].

To evaluate these impacts systematically, Life Cycle Assessment (LCA) has emerged as the principal method for quantifying the environmental performance of the built environment across its cradle-to-grave stages [10]. However, executing rigorous, whole-building LCA within emerging tropical administrative capitals faces substantial methodological and operational bottlenecks [22, 23]. Conventional building LCAs frequently rely on disconnected, static spreadsheets or retrospective analyses after architectural designs are finalized, preventing architects and structural engineers from identifying carbon-intensive material hotspots during early design stages [3, 24]. While Building Information Modelling (BIM) offers automated material quantity take-offs (QTO) to streamline LCI compilation, many digital integrations suffer from poor interoperability, unstandardized classification frameworks, and inconsistent system boundaries [3, 25]. Moreover, the structural lifespan and temporal boundary selected for high-density administrative facilities are often arbitrary [22, 26]. In dynamic public sectors, short-to-medium analytical horizons (e.g., a 20-year boundary corresponding to national decarbonization milestones) sharply compress the operational amortization window, elevating the relative significance of upfront material manufacturing relative to cumulative operating emissions [10, 26]. Then, many emerging regions lack localized LCI databases, compelling practitioners to adapt international datasets without accounting for regional industrial supply chains, material transportation profiles, or local grid emission factors [10, 23]. Finally, building LCA studies routinely suffer from severe parametric and model uncertainty [27, 28]. Conventional local, one-at-a-time (OAT) sensitivity analyses fail to account for non-linear interactions and simultaneous multi-parameter variations across structural, envelope, and operational domains [27]. While variance-based GSA – specifically variance decomposition via first-order and total-order Sobol indices – provides a mathematically robust framework for identifying critical input drivers and interaction effects, its explicit integration within high-rise tropical building LCAs remains exceedingly rare [28].

Simultaneously, renewable energy generation integrated directly into building surfaces represents an essential strategy for offsetting remaining operational loads [29, 30]. Building-Integrated Photovoltaics (BIPV) transforms passive building envelopes into active solar energy generators, offsetting fossil-fuel grid electricity while providing daylighting and solar heat gain control [11, 31]. In tropical equatorial environments with abundant solar irradiance, such as East Kalimantan, high solar radiation intensity offers strong solar yields [32, 33]. Nevertheless, elevated ambient temperatures induce thermal degradation in crystalline silicon solar cells (a 1 °C temperature rise typically reduces power output by 0.4% to 0.5%), necessitating specialized ventilation cavities, optimal orientation, and careful techno-economic lifecycle appraisal [11, 29, 34]. Furthermore, deploying on-site BIPV must be evaluated alongside life cycle costing (LCC), net present value (NPV), and energy payback time (EPBT) to ensure that capital-intensive renewable interventions remain financially viable over the asset lifespan [34, 35].

To address these interconnected challenges, this paper presents a novel, integrated BIM–LCA–GSA Decarbonization Framework tailored specifically for high-rise institutional buildings in tropical master-planned capital cities. By bridging digital architectural modelling, localized whole-life environmental accounting, and rigorous variance-based sensitivity modelling, this research provides the first comprehensive life-cycle decarbonization assessment for a public administrative high-rise building situated in Nusantara (IKN), Indonesia. The primary goals of this study are structured across four main dimensions:

1. Establishing a high-resolution, cradle-to-grave Life Cycle Inventory (LCI) through BIM extraction to evaluate the relative shares of Embodied Carbon (EC) and Operational Carbon (OC) over a targeted 20-year operational horizon; this specific timeframe is justified by current regulatory uncertainties in Indonesia's new capital and the realistic possibility that early-phase building service lives may not reach the conventional 50-year average, ultimately clarifying the shifting dominance of material manufacturing over operational electricity in modern energy-efficient tropical construction.
2. Formulating and evaluating deep decarbonization pathways, including high-volume industrial supplementary cementitious materials and high-performance façade configurations to identify structural material carbon reduction potentials.
3. Coupling 3D building geometry with dynamic meteorological simulations to assess on-site solar generation capability, energy payback periods, and economic viability over the building's operational lifespan.
4. Applying a probabilistic Monte Carlo simulation combined with Sobol indices to quantitatively rank input parameter uncertainty, defining which structural and operational parameters govern the majority of output GWP variance to provide design teams with an empirical risk-management tool.

Methodology and Methods

Methodological Framework

This study uses computer simulation and quantitative assessment to evaluate life cycle carbon emissions and BIPV retrofit performance in a high-rise residential building in Nusantara. The framework executes five sequential steps: (1) defining the goal, scope, functional unit, and system boundary; (2) developing the LCI via BIM extraction; (3) calculating life cycle impacts in kg CO_2e; (4) interpreting baseline results via hotspot and Global Sensitivity Analysis (GSA); and (5) modelling BIPV retrofit scenarios to compare techno-economic and decarbonization performance against the baseline. Figure 1 presents the workflow from LCI development to LCIA, sensitivity analysis, PV modelling, and scenario comparison.

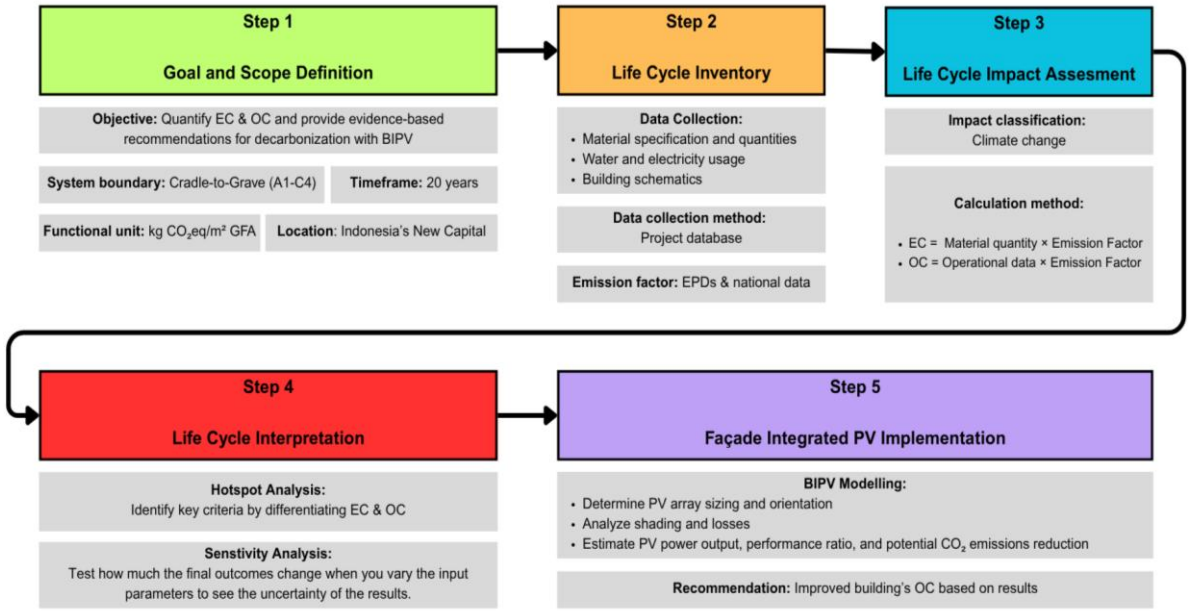


Figure 1. Research methodology framework

Study Location and Case Building

The case building is a 12-storey residential tower in Nusantara, Indonesia. The building has a gross floor area (GFA) of 11,667 m^2, featuring 60 apartment units and two lower floors for commercial and shared functions. Each unit is designed for two occupants, yielding an assumed occupancy of 120 residents based on standard volumetric design capacities. Construction commenced in August 2023 and concluded in March 2025, with operations beginning immediately thereafter. The projected annual electricity demand is 451 MWh/year. Figure 2 below displays the delineation of the Nusantara development area.

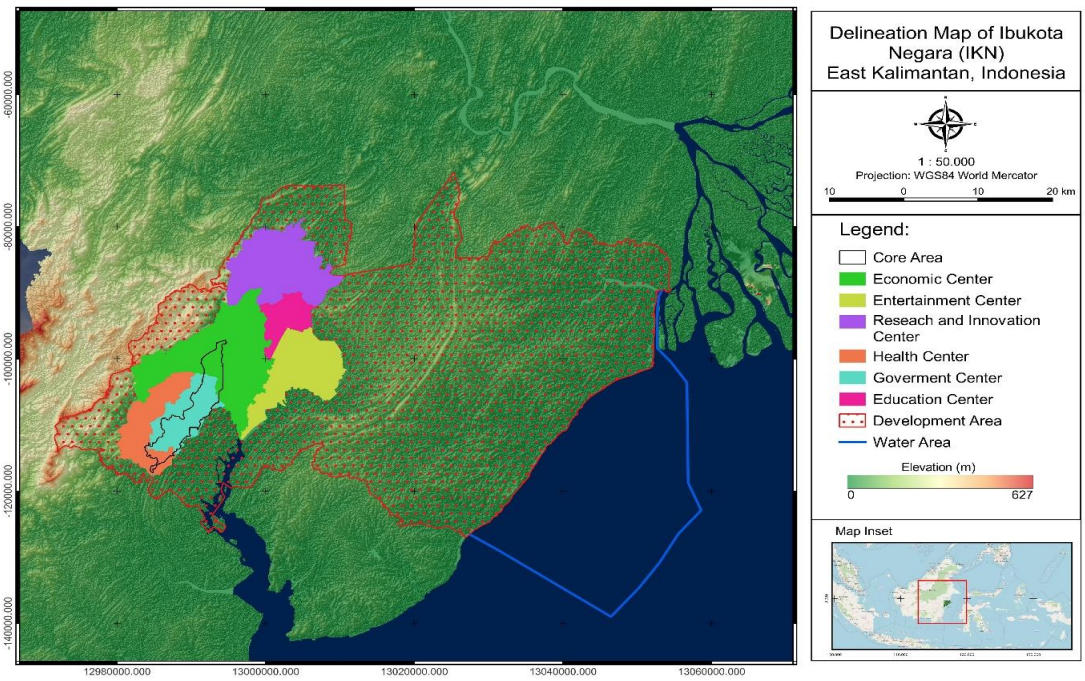


Figure 2. Location of Indonesia's New Capital (Nusantara)

The selected building typifies the high-density vertical housing prioritized in Nusantara's urban development strategy [7]. Because high-rise residential buildings possess limited rooftop areas relative to their GFA, conventional rooftop PV systems face inherent spatial constraints, making façade-based BIPV a critical alternative for assessment.

LCA Framework and Boundary

The LCA is conducted utilizing One Click LCA, a tool compliant with EN 15978:2011 standard workflows that facilitates manual inventory input, BIM integration, and Environmental Product Declaration (EPD) mapping [23]. The system boundary is strictly defined as "Cradle-to-Grave" (Figure 3), encompassing the product stage (Modules A1–A3), construction stage (Modules A4–A5), use stage (Modules B1–B7), and end-of-life (EOL) stage (Modules C1–C4).

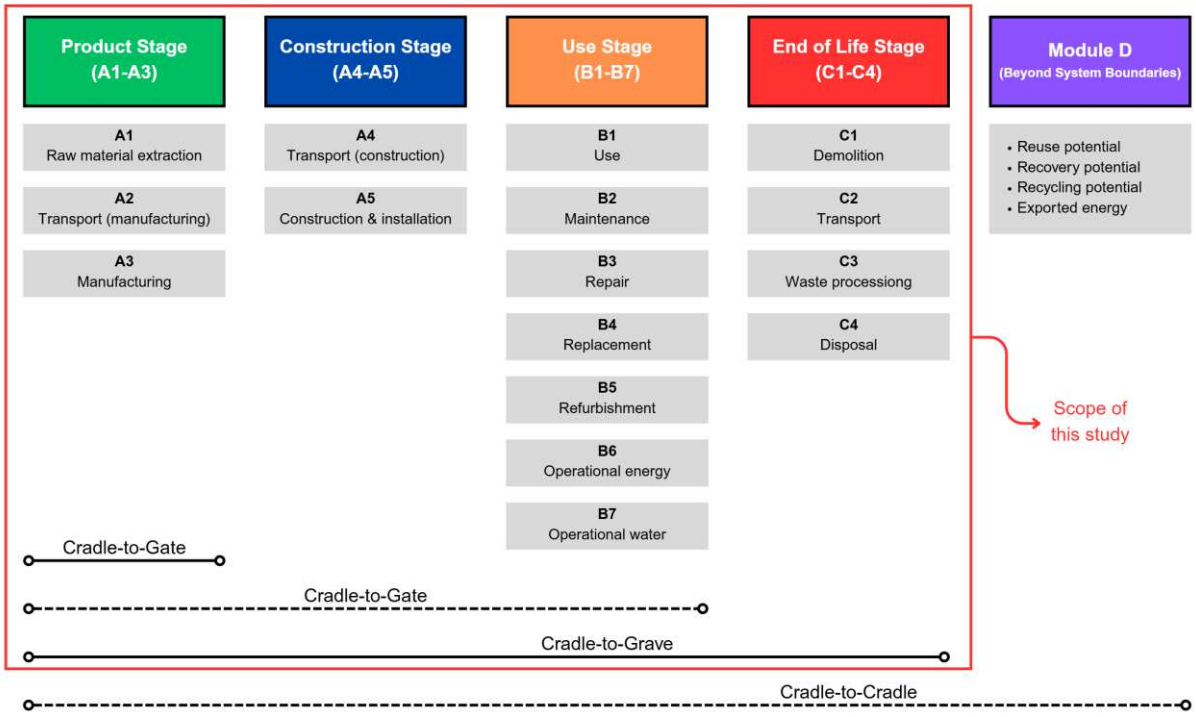


Figure 3. LCA boundary of this study

While building LCAs conventionally assume a 50-year service life, this 20-year temporal boundary is explicitly chosen to align with the Indonesian Capital Authority's 2045 NZE mandate. This specific timeframe is further justified by profound financial and regulatory uncertainties surrounding Indonesia's new capital following a recent shift in national leadership. As state budget prioritization pivots heavily toward massive social and security programs – including an escalating allocation of up to Rp 335 trillion for free nutritious meals (MBG) by 2026, alongside extensive funding for defense (Rp 145 trillion), police (Rp 125 trillion), and subsidized housing (Rp 43 trillion) – fiscal resources for mega-infrastructure projects are increasingly constrained [36]. This macro-economic reallocation introduces the realistic possibility that early-phase buildings in the new capital may face stalled development, repurposing, or major structural refits well before reaching the conventional 50-year average service life. Furthermore, a 20-year boundary compresses the operational amortization window, strictly stress-testing the upfront embodied carbon limits and preventing reliance on delayed compliance [22, 26].

Life Cycle Inventory (LCI) and Data Blending

The LCI phase involves the systematic collection and quantification of material and energy flows. Data was sourced from as-built construction documents and precise material take-offs. Due to the scarcity of localized EPDs within the Indonesian context, a data blending approach was adopted to map the inventory. Where specific Indonesian datasets were unavailable, the closest available proxy entries from international databases (e.g., China, India, and the broader APAC region) were utilized. To maintain regional accuracy despite this substitution, transportation emissions (Module A4) were manually adjusted for all imported materials, assuming maritime freight to the local Balikpapan port prior to truck delivery to the site.

For the use phase (Module B), structural materials are assumed to last the full 20-year study period without replacement, with the exception of architectural paint and weather shielding, which operate on a 10-year replacement cycle. The EC and OC are calculated based on the following equations [14].

Life Cycle Impact Assessment (LCIA) and Interpretation

The LCIA quantifies the GWP of the building across all modules. EC is calculated by multiplying material quantities by their respective EPD emission factors, while OC is derived by multiplying annual grid electricity and water consumption by the localized Indonesian energy emission factor (calculated implicitly as 0.946 kg CO_2e/kWh. The emissions are calculated following Equations 1 and 2.

a) EC emissions

$$EC_{building} = \Sigma(Q_i \times EF_i) \quad (1)$$

Note:

- Q_i = Quantity of material i (e.g., m^2, m^3, or kg)
- EF_i = Emission factor for material i (kg CO_2-eq/unit)

b) OC emissions

$$OC_{building} = E_i \times EF_i \quad (2)$$

Note:

- E_i = Consumption of energy source i (e.g., kWh, m^3)
- EF_i = Energy emission factor for source i in Indonesia (kg CO_2-eq/unit)

LCA Global Sensitivity Analysis (GSA)

To address the parametric uncertainties inherent in LCI blending and operational projections, a GSA is applied. The study uses variance-based Sobol indices combined with a 1,000-run Monte Carlo simulation (Kim et al., 2025). The two primary indices utilized are the first-order index (S_I) and the total-order index (S_T), defined mathematically as:

$$S_1(x_i) = \frac{Var[E(y|x_i)]}{Var_y} \quad (3)$$

$$S_T(x_i) = \frac{Var[E(y|x_j, j \neq i)]}{Var_y} \quad (4)$$

Note:

- $S_1(x_i)$ = The first-order Sobol index, measures the direct contribution of one input to output variance.

- $S_T(x_i)$ = The total-order Sobol index, measures the total contribution of one input, including interaction effects with other inputs.
- Var_y = The total variance of the model's output when all input parameters are varying. This represents the total uncertainty in the result.
- $E(y|x_i)$ = The expected value (or average) of the output y when the input parameter x_i is held constant, while all other parameters are allowed to vary.
- $Var[E(y|x_i)]$ = The variance of that expected value. It measures how much the average output changes solely due to variations in x_i.
- $Var[E(y|x_j, j \neq i)]$ = The expected value (or average) of that remaining variance, calculated across the full range of all other parameters. This gives a total measure of the influence of x_i.

In practical terms for interpreting the LCA results, the first-order index (S_I) represents the direct reduction in output variance (uncertainty) that would be achieved if a specific input parameter could be perfectly determined. Conversely, the total-order index (S_T) captures the total influence of a parameter, including all variance caused by its non-linear interactions with other variables in the building system. Therefore, parameters exhibiting a high S_T indicate that the building's total carbon footprint is highly volatile depending on that specific input, prioritizing it as a critical target for design mitigation or data quality improvement [37, 38] .

BIPV Modelling, Simulation, and Economic Assumptions

To model the PV array sizing, orientation, system losses, and annual energy yields, PVsyst 8 was selected. As per comparative assessments of simulation tools, PVsyst offers superior advanced loss modelling and proven accuracy for façade-integrated systems compared to other generic building simulation platforms [39] .
The solar resource evaluation utilized three Typical Meteorological Year (TMY) datasets: Meteonorm, PVGIS ERA5, and NREL NSRDB. For the primary techno-economic baseline, Meteonorm was selected over PVGIS and NREL. This selection is objectively justified by prior validation studies in Southeast Asian equatorial regions, which demonstrate that Meteonorm exhibits lower Mean Bias Error (MBE) and tighter Root Mean Square Error (RMSE) distributions for Global Horizontal Irradiance (GHI) when compared to concurrent ground-station measurements under highly variable tropical cloud cover [32, 33].
Two hybrid BIPV scenarios were modeled, combining standard rooftop installations with vertical façade integrations (Table 3), incorporating specific optical and system losses outlined in Table 4.

Table 3. BIPV scenario definition

Array Type	Scenario 1	Scenario 2	Module Model
Rooftop PV (Array #1)	31.7 kWp (48 modules)	63.4 kWp (96 modules)	LR7-72HYD-660M
BIPV (Array #2 – North façade)	5.92 kWp (32 modules)	5.92 kWp (32 modules)	
BIPV (Array #3 – East façade)	8.88 kWp (48 modules)	8.88 kWp (48 modules)	FLEX60-185W-M20-A
BIPV (Array #4 – South façade)	N/A	5.92 kWp (32 modules)	
BIPV (Array #5 – West façade)	N/A	8.88 kWp (48 modules)	
Total System Power	46.5 kWp	93.0 kWp	

The façade BIPV modules are vertical, with a tilt angle of 90°. Scenario 1 places modules on the north façade with an azimuth of -10° and east façade with an azimuth of -100°. Scenario 2 adds modules on the south façade with an azimuth of 170° and west façade with an azimuth of 80°.

Table 4. Assumed Losses for Vertical BIPV

Optical Losses	System Losses
a) Incidence Angle Modifier (IAM) using Fresnel equations (n=1.526)	a) Temperature losses (Uc = 29.0 W/m^{2}K, Uv = 0.0 W/m^{2}K/m/s)
b) Near shading from building elements (linear shading method)	b) DC wiring losses: 1.50% at STC
c) Soiling losses: 3.0% (urban environment)	c) Module mismatch: 2.00% at MPP
d) Diffuse and albedo factors: 0.003 to 3.0	d) Module quality loss: –0.75%
	e) String mismatch: 0.05%

Ultimately, PV performance indicators follow IEC 61724-1 and methodologies used in measuring and simulating the performance of a grid-connected PV system in eastern India [NO_PRINTED_FORM] [40]. The study calculates array yield, reference yield, final yield, and performance ratio.

a) Array Yield (Y_A) [h/day]

$$Y_A = \frac{EDC}{P_{pv\,rated}} \quad (5)$$

Where:

- EDC = DC energy output from a PV array over a particular period (kWh/day)
- $P_{pv\ rated}$ = PV rated power (kW)

b) Reference Yield (Y_R) [h/day]

$$Y_R = \frac{H_t}{G_0} \quad (6)$$

Where:

- H_t = Total in-plane irradiance (kWh/m^2/day)
- G_0 = PV's reference irradiance (kW/m^2)

c) Energy Yield (Y_F) [kWh/year]

$$Y_F = \frac{E_{AC}}{P_{rated}} \quad (7)$$

Where:

- E_{AC} = Annual net Alternating Current (AC) energy output of the PV system (kWh/year)
- P_{rated} = Installed peak power at STC with solar irradiance of 1 kW/m^2 at 25 °C

d) Performance Ratio (PR)

$$PR = \frac{Y_F}{Y_R} \quad (8)$$

To assess economic viability, conservative financial parameters were deliberately chosen. The assessment assumes a static electricity tariff of AUD 0.14/kWh, a 5.5% annual discount rate (i), and crucially, the absence of a feed-in tariff. By relying purely on self-consumption savings rather than external subsidies, the financial model prevents the overestimation of economic returns [35].

e) Payback period

$$PP = \frac{I_i}{AC} \quad (9)$$

Where:

- I_i = Initial investment (AUD)
- AC = Annual cash flow (AUD/year)

f) Net present value (NPV)

$$NPV = \sum_{t=0}^{n} \frac{R_t}{(1+i)^t} \quad (10)$$

Where:

- R_t = Net cash flow for each period t
- i = Discount rate (5.5%/year)
- n = total number of periods

Results and Analysis

Life Cycle Inventory and LCA Results

The building has a gross floor area (GFA) of 11,667 m^2 throughout its 12-storey structure, where two levels serve as commercial and common areas, while the remaining 10 levels are designed for residential purposes. There are 60 apartment units in total, where each unit has 2 occupants. The building has a mixed frame consisting of concrete supported by steel rebar. The building's annual energy demand is projected to be ±451,275.5 kWh/year. The assessment period is 20 years, from building operation in 2025 to the 2045 net-zero target year for Nusantara. The detailed material quantities are outlined in Table 5.

Table 5. Building Materials Quantity and Operational Data, in BaU Scenario

Category	Materials	EPD number	Quantity	Unit	Global Warming Potential (kg CO_2e/unit)	Country of Origin	Transport Distance (km)	Mode of transport
Steel	Steel rebar	S-P-13603	1,299,817	kg	2.61	Indonesia	1,879	Vessel, truck
	Hot rolled coil	EPD-IES-0019977:002	37,234.09	kg	2.26	Indonesia	1,879	Vessel, truck
Concrete	Ready-mix lightweight aggregate concrete, LC30	N/A*	6,537	m^3	446.51	Indonesia	10	Truck
	Prestressed concrete pile	N/A*	851	m^2	113.6	Indonesia	60	Truck
	Anchor bolt for concrete element	NEPD-4427-3691-EN	2,804	m^2	1.57	China	3,980	Vessel, truck
	Exposed aggregate concrete pavers for outdoor application	N/A*	3,842	m^2	17.2	Indonesia	10	Truck
Construction activities	Average site impacts - world average climate (per GFA)	N/A*	11,666.67	m^2	36.45	N/A	N/A	N/A
	Machine hours	N/A*	9,240	hours	93	N/A	N/A	N/A
	Excavator operation per 1 m^3 of excavated earth mass	N/A*	5,595.45	m^3	0.26	N/A	N/A	N/A
	Deconstruction/demolition scenarios	N/A*	11,666.67	m^2	5.43	N/A	N/A	N/A
External façades	Galvanized steel railing	INIES_IWJS20230719_092323, 34628	41	m	1.4	Spain	12,636	Aircraft, truck
	Tempered glass	EPD-IES-0017729:001	120	m^2	11.3	China	3,031	Vessel, truck
	uPVC window with insulating foam	N/A*	120	m^2	91.81	Indonesia	75	Truck
	Water repellent paints and coatings	N/A*	5,643	m^2	1.83	Indonesia	92	Truck
	PVC cladding board for walls and façades	HUB-3309	1,485	m^2	49.3	China	3,624	Vessel, truck
Other materials	Interior acrylic emulsion paint	NEPD-4652-3951-EN	23,081.38	m^2	2.16	Indonesia	10	Truck
	Floor tiling	S-P-10515	1,032	m^2	8.56	Philippines	1,803	Vessel, truck
	Gypsum board (water resistance)	EPD-IES-09820	1,172	m^2	2.47	India	4,351	Vessel, truck
	Insulated glass panes	EPD-IES-0017432:001	656.82	m^2	52.4	China	4,600	Vessel, truck
	Insulated glass unit	EPD-IES-0017733:001	1,900	m^2	25.1	China	3,624	Vessel, truck
	Plywood panels	EPD-IES-0016070:001	313	pcs	27.4	China	3,980	Vessel, truck
	Lever handles	EPD-DOR-20240262-CBA1	313	pcs	4.55	China	3,980	Vessel, truck
	Aliphatic acrylic polyurethane finish	S-P-07099	375.5	m^2	0.99	Indonesia	470	Vessel, truck
	Office cubicle separation wall	N/A*	13	pcs	308.4	Indonesia	320	Vessel, truck
	Cement-based waterproofing coating with polymer additives	EPD-IES-0016400:001	5,353.24	kg	0.67	Singapore	1,946	Vessel, truck
Water usage	Tap water, conventionally treated	N/A*	9,836	m^3	3.0E-4	N/A	N/A	N/A
Electricity usage	Electricity, Indonesia	N/A*	451,275.5	kWh	0.95	N/A	N/A	N/A

*From One Click LCA® EPD Program

Supplier-specific freight records were not available. Therefore, the A4 results represent modelled transport emissions from One Click LCA and selected EPD entries. Imported products were treated using their database transport entries, with an added explanation for final domestic delivery through Balikpapan. This avoids false precision while making the transport assumption transparent. The LCIA is conducted to get a Business as Usual (BaU) result from the LCI data in Table 5. This baseline scenario reveals a total emissions of 1.73×10^7 kg CO_2e. Operational electricity was the largest single source, with 8.53×10^6 kg CO_2e, equal to 49.3% of the total. The implied grid emission factor was 0.946 kg CO_2e/kWh. This value was calculated by dividing the 20-year operational electricity emissions by the annual electricity demand and the 20-year assessment period. The overall baseline emissions are presented in Table 6.

Product-stage emissions from A1–A3 reached 6.79×10^6 kg CO_2e, equal to 39.2% of total emissions. Construction-stage emissions from A5 reached 1.60×10^6 kg CO_2e, equal to 9.2%. Transport to site under A4 contributed 0.112 $\times 10^6$ kg CO_2e, equal to 0.65%. End-of-life stages contributed 0.199×10^6 kg CO_2e, equal to 1.15%. This confirms two main hotspots: operational electricity and structural materials.

Table 6. LCA Results over 20-year assessment period

Phase	BaU GWP (kg CO_2e)	Scenario 1 GWP (kg CO_2e)	Scenario 2 GWP (kg CO_2e)	Notes
Product stage (A1–A3)	6,788,560	6,822,631	6,890,514	Product-stage emissions increased due to additional PV panels.
Transport (A4)	112,196	112,252	112,365	Transport emissions changed slightly because PV transport adds a small load.
Construction (A5)	1,597,042	1,597,042	1,597,042	Construction activity assumptions stayed constant across scenarios.
Replacement (B4–B5)	17,356	17,356	17,356	Replacement assumptions stayed constant.
Operational electricity (B6)	8,534,760	7,608,395	6,615,298	PV generation reduced grid electricity demand.
Operational water (B7)	53,309	53,309	53,309	Water use stayed constant across scenarios.
End of life (C1–C4)	198,896	198,976	199,135	End-of-life emissions increased slightly due to added PV materials.
Total	**17,302,119**	**16,409,961**	**15,485,018**	

The product-stage result was dominated by steel and concrete. Reinforcement steel alone produced 3.30×10^6 kg CO_2e, equal to 48.6% of A1–A3 emissions. Ready-mix lightweight aggregate concrete produced 3.00×10^6 kg CO_2e, equal to 44.2% of A1–A3 emissions. Together, these two materials explained 92.8% of product-stage emissions. This result shows why the building's carbon profile depends strongly on structural material selection.

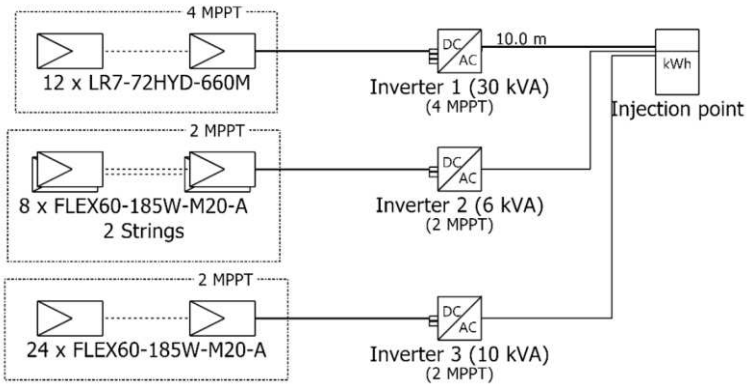
The BaU scenario shows a near-even split between embodied carbon and operational carbon. Embodied carbon reached 8.71×10^6 kg CO_2e, equal to 50.4% of total life cycle emissions. Operational carbon reached 8.59×10^6 kg CO_2e, equal to 49.6%. This differs from many tropical building studies where operational energy usually dominates due to cooling demand [14, 16].

The result mainly reflects the short 20-year assessment period and the high structural material intensity of the 12-storey building. A longer assessment period would increase the relative share of operational carbon because electricity use accumulates each year. Within the 20-year boundary used in this study, the upfront emissions from steel, concrete, and construction activities remain substantial.

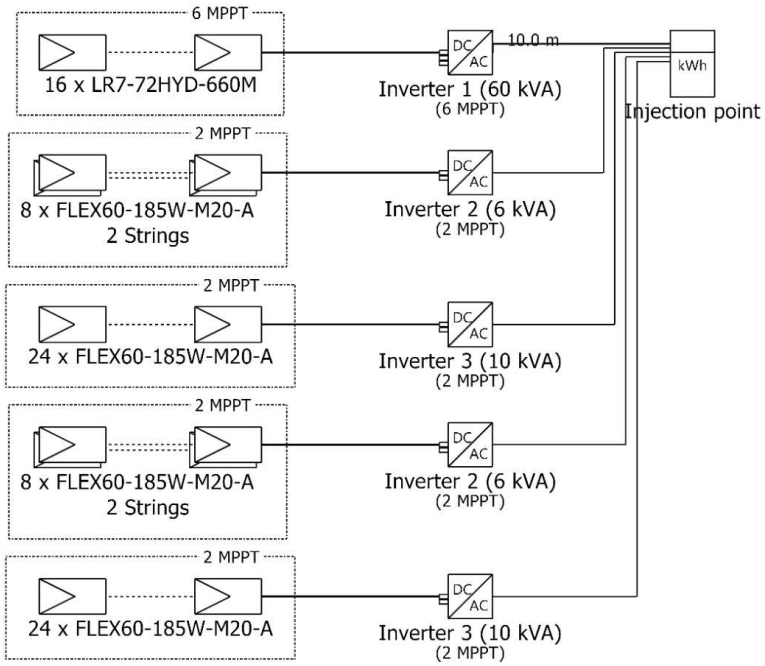
BIPV Scenario Results

After the baseline LCA result is obtained, the BIPV retrofit is then modelled. The model includes a hybrid photovoltaic (PV) system that combines a standard rooftop installation with a facade-integrated BIPV system. There are two scenarios designed with different array capacities. The total nominal power of this first scenario is 46.5 kWp, comprising 128 modules covering an area of 261 m^2. The existing rooftop PV array provides most of the capacity, with a nominal power of 31.7 kWp. For the second scenario, the total nominal power is 93 kWp, consisting of 256 modules in an area of 522 m^2 – twice the size of the first scenario. The PV system configuration is described in

The BIPV system from scenario 1 has a total capacity of 14.8 kWp and is split into two separate arrays on the building's façade to improve solar irradiance collection throughout the day. The first BIPV array is on the north-facing façade and has a capacity of 5.92 kWp, consisting of 32 modules arranged vertically at a 90° tilt with a –10° azimuth. The second, larger BIPV array is on the east-facing façade, providing 8.88 kWp from 48 modules, also installed vertically at a 90° tilt with a –100° azimuth. Then, for scenario 2, there is an additional 31.7 kWp rooftop PV, 5.92 kWp BIPV on the south-facing façade (90° tilt, 170° azimuth), and 8.88 kWp BIPV on the west-facing façade (90° tilt, 80° azimuth). The Single-line diagram of the BIPV system for both scenarios is illustrated in Figure 4 below.



(a)



(b)

Figure 4. Single-Line Diagram for: (a) Scenario 1; (b) Scenario 2

The useful energy output modelled from the BIPV system with Meteonorm, NREL, and PVGIS TMY data is displayed in Figure 4 below. Scenario 1 has a daily useful energy of 145.29 kWh/day (Meteonorm), 143.47 kWh/day (NREL), and 135.44 kWh/day (PVGIS). On the other hand, scenario 2 has a daily useful energy of 290.88 kWh/day (Meteonorm), 287.27 kWh/day (NREL), and 271.17 kWh/day (PVGIS). Both scenarios follow a similar pattern of energy output, with notable differences in variability. Scenario 2 has more variability in energy output compared to scenario 1, with a noticeable, near-zero value in June–August, and >400 kWh/day generation at times throughout the year. The Meteonorm power output is noticeably better compared to PVGIS and NREL, and hence will be used for further analysis of the PV system.

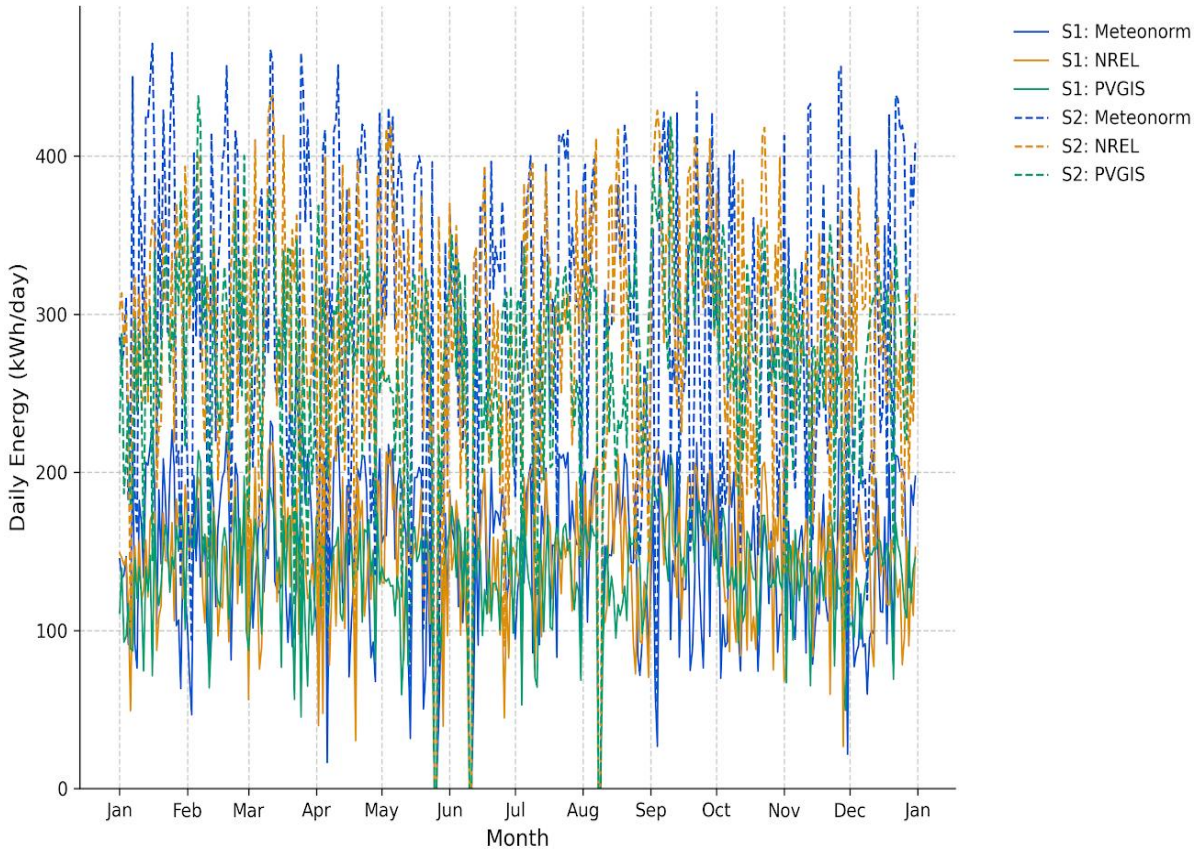
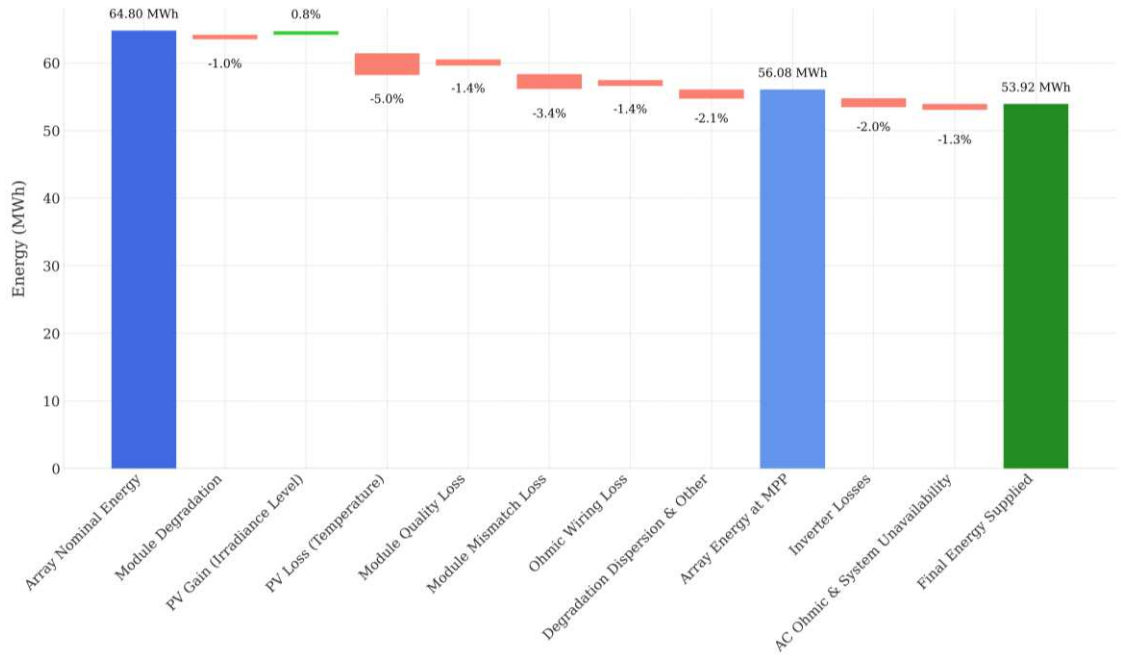
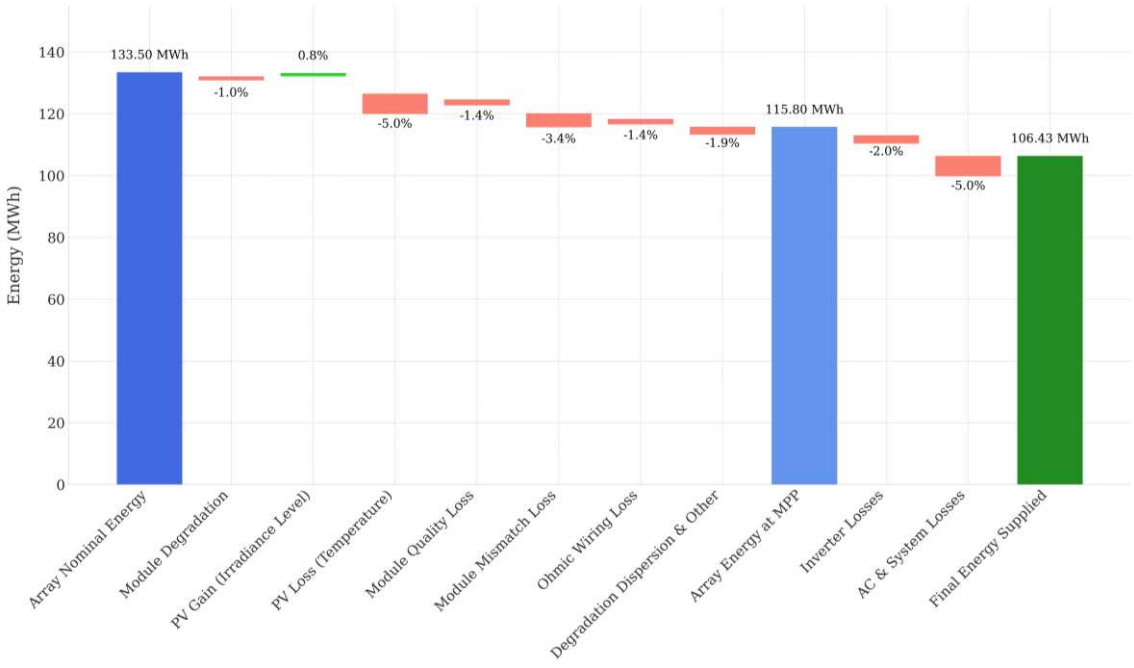


Figure 5. PV system energy output throughout a calendar year period

The combined rooftop and BIPV system is expected to generate 53.92 MWh and 106.43 MWh of useful energy annually for scenario 1 and scenario 2, respectively. The achieved specific production rate for both scenarios is 1160 kWh/kWp/year and 1145 kWh/kWp/year, respectively. The energy loss analysis, shown in Figure 5, illustrates the step-by-step decline from the system's theoretical potential to its actual energy output. It starts with a calculated Array Nominal Energy of 64.80 MWh (scenario 1) and 127.16 MWh (scenario 2), which represents the maximum possible generation under Standard Test Conditions (STC). Several factors lower performance at the array level. The most significant is the PV Loss due to temperature, which reduces energy yield by 5.0%. Other major reductions at the array level include Module Mismatch Loss of –3.4% and various smaller losses from module quality, degradation, and ohmic resistance. After accounting for these total DC-side losses, the energy produced by the array at its Maximum Power Point (Array Energy at MPP) is reduced to 56.08 MWh (scenario 1) and 115.8 MWh (scenario 2).



(a)



(b)

Figure 6. Detailed PV system energy loss analysis: (a) Scenario 1; (b) Scenario 2 – The largest loss occurs in the temperature loss and module mismatch loss

After the initial generation phase, more losses happen during power conversion and delivery. The 56.08 MWh (scenario 1) and 115.8 MWh (scenario 2) of DC energy experience Inverter Losses of –2.0% during their conversion to AC electricity. This reduction is due to the efficiency limits of the power electronics. The final losses are caused by AC & System Losses of –1.3%, which include ohmic losses in the AC wiring and periods when the system is unavailable. Thus, after accounting for all these thermal, material, conversion, and systemic inefficiencies, the Final Energy Supplied to the building's electrical system is 53.92 MWh (scenario 1) and 106.43 MWh (scenario 2).

The overall system Performance Ratio (PR) of 77.64% (scenario 1) and 76.61% (scenario 2) is shown in Figure 6. Both scenarios show a consistent performance throughout the year, with scenario 2 having a slightly worse

performance of 1.03%. The worst-performing month was seen to occur in February, which is not that far from the best-performing month in Aug, with a difference of only 10.7%.

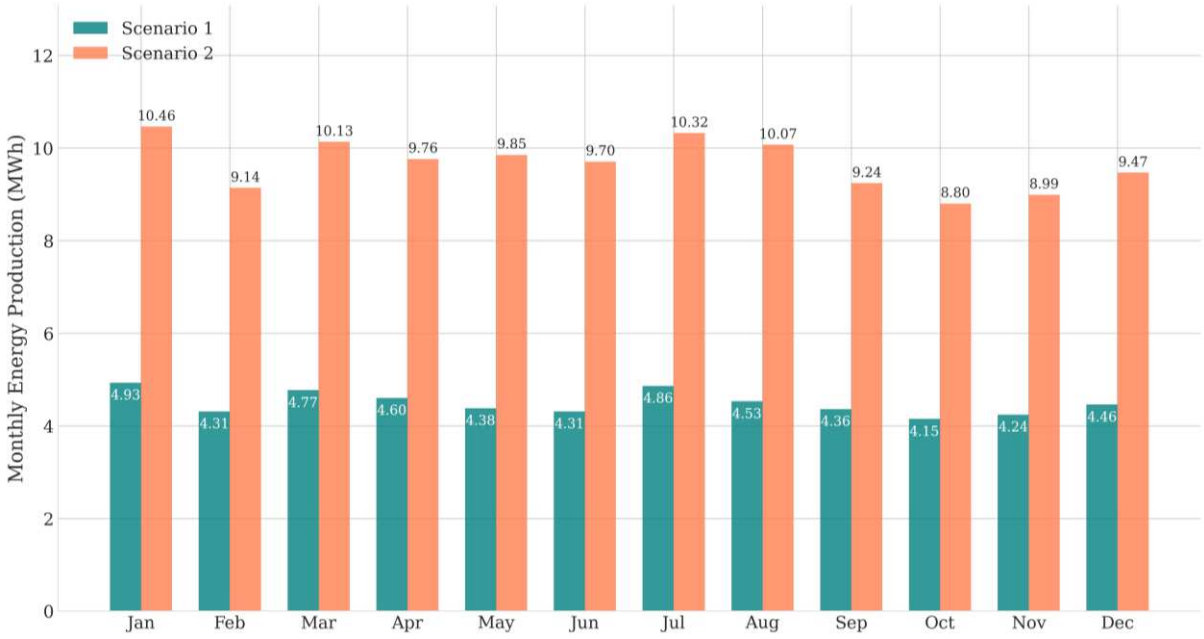


Figure 7. BIPV Performance Summary

Scenario Analysis, Based on Material and Activity Types

The Business as Usual (BaU) and two BIPV retrofit scenarios were analyzed within the 20-year assessment period, summarized in Table 7. These retrofit scenarios lead to a significant 10.9% and 22.5% reduction in carbon emissions from electricity use, cutting emissions by 0.926×10^6 kg CO_2e (scenario 1) and 1.919×10^6 kg CO_2e (scenario 2). On the other hand, the embodied carbon profile shows a small increase in the "Other materials" category, going up by 0.34×10^5 kg CO_2e (scenario 1) and 1.02×10^5 kg CO_2e (scenario 2). This rise is caused by the production and installation of BIPV components.

Table 7. Carbon emissions of BaU and BIPV Retrofitted Scenarios (measured in kg CO_2e) calculated from as-built data

Component	Business as Usual (kg CO_2e)	Scenario 1 (kg CO_2e)	Scenario 2 (kg CO_2e)	Scenario 1 Reduction (kg CO_2e)	Scenario 1 Reduction (%)	Scenario 2 Reduction (kg CO_2e)	Scenario 2 Reduction (%)
Embodied Carbon							
Steel	3.706×10^6	3.706×10^6	3.706×10^6	0	0.0%	0	0.0%
Concrete	3.394×10^6	3.394×10^6	3.394×10^6	0	0.0%	0	0.0%
Construction activities	1.349×10^6	1.349×10^6	1.349×10^6	0	0.0%	0	0.0%
External façades	1.06×10^5	1.06×10^5	1.06×10^5	0	0.0%	0	0.0%
Other materials	1.55×10^5	1.66×10^5	2.27×10^5	-0.11×10^5	–7.1%	-0.61×10^5	–39.4%
Operational Carbon							
Energy (electricity)	8.534×10^6	7.608×10^6	6.615×10^6	0.926×10^6	10.9%	1.919×10^6	22.5%
Water	0.53×10^5	0.53×10^5	0.53×10^5	0	0.0%	0	0.0%
Total	1.73×10^7	1.64×10^7	1.55×10^7	0.895×10^6	5.2%	1.817×10^6	10.5%

However, this small increase in embodied carbon is more than balanced by the savings in operational carbon. As a result, the retrofitted scenarios achieve a total net reduction of 0.895×10^6 kg CO_2e (scenario 1) and 1.817×10^6 kg CO_2e (scenario 2), which is a 5.2% and 10.5% decrease in the building's total carbon emissions compared to the BaU case. This reduction further leads to reduced overall emissions by the EoL phase from 1.73×10^7 kg CO_2e (BaU) to 1.64×10^7 kg CO_2e (scenario 1) and 1.55×10^7 kg CO_2e (scenario 2), illustrated in Figure 8.

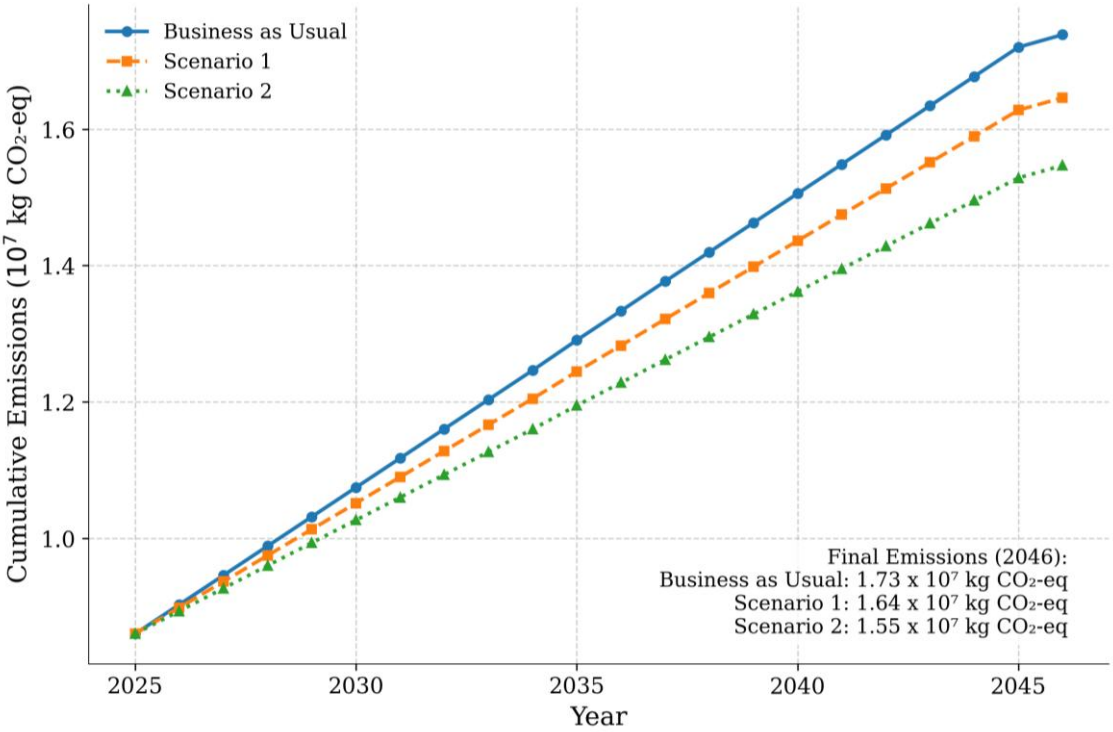


Figure 9. Cumulative Life Cycle Emissions (2025–2046) – The extra one year beyond 2045 indicates the EoL phase

Figure 9 shows that the drop in Global Warming Potential (GWP) mainly comes from lower emissions from electricity use. The GWP linked to primary structural components (i.e., concrete, steel, construction activities, and external façades) stays consistent between the two scenarios. The separation between the pathways increases over time because PV generation offsets grid electricity every year.

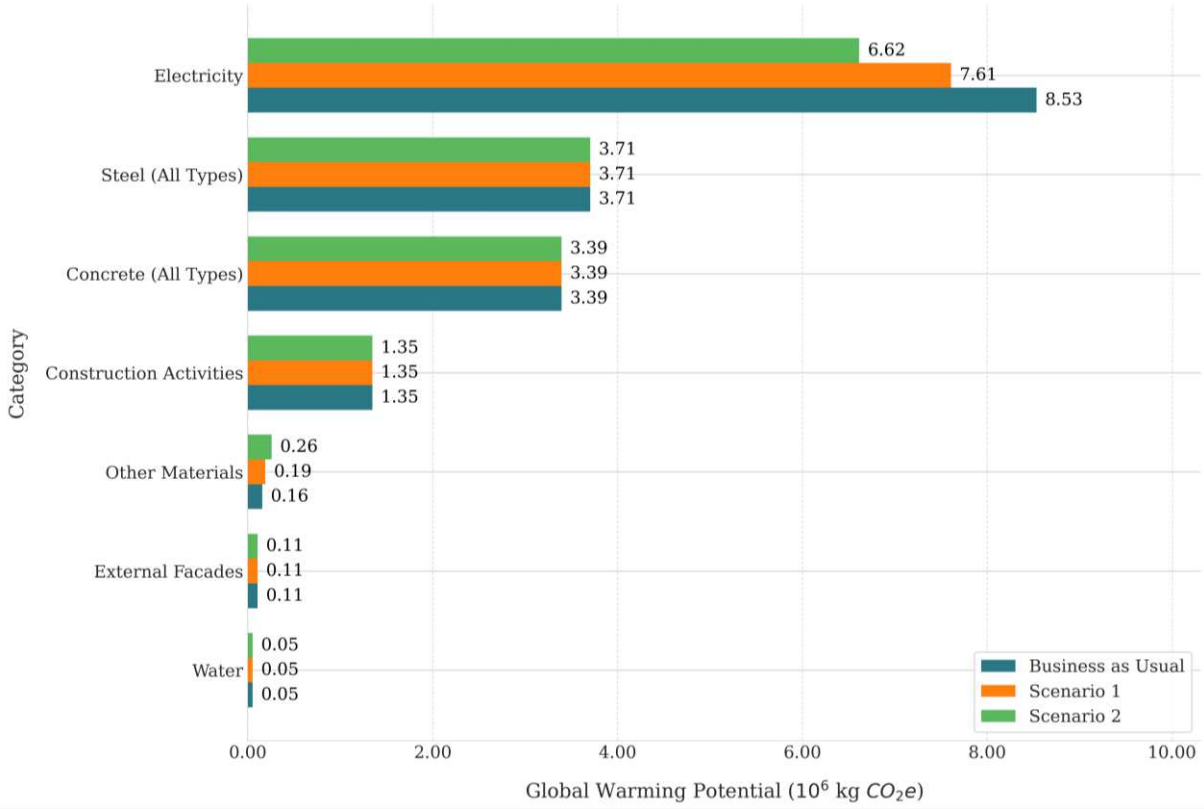


Figure 10. Detailed GWP comparison by material and process categories

The main change, illustrated in Figure 10, occurs in the operational electricity (B6 phase). Other stages and building materials change only slightly because the building structure, water usage, replacement cycle, and construction assumptions remain constant across scenarios. This result confirms that BIPV mainly affects OC, while structural materials remain EC hotspot.

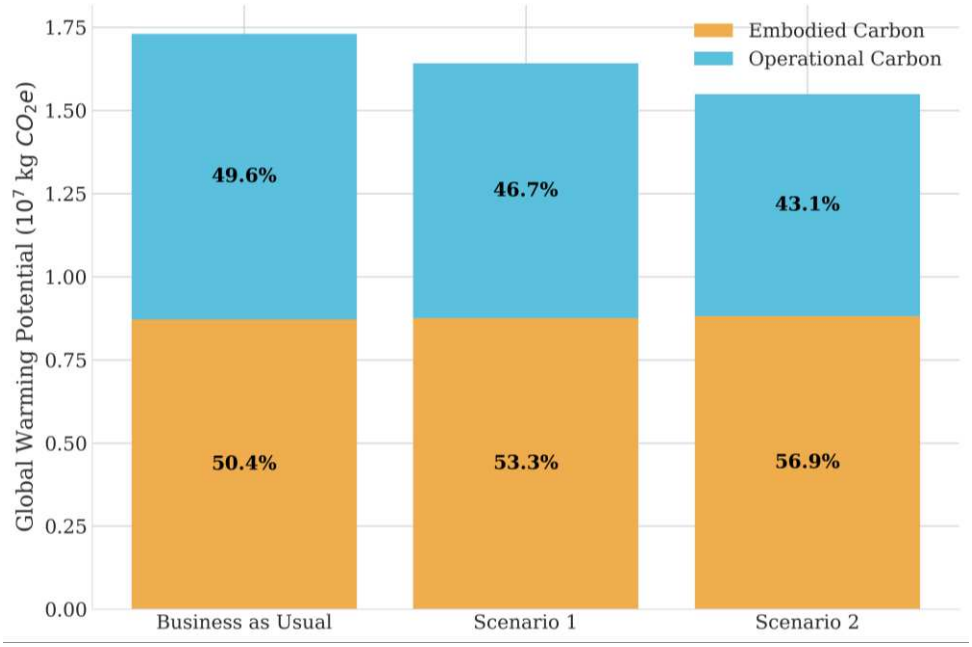


Figure 11. EC and OC composition between the BaU and retrofit scenarios

Furthermore, the composition of building lifecycle GWP shifted to 53.3% OC and 46.7% EC in scenario 1. For scenario 2, the EC and OC contributed 56.9% and 43.1% of lifecycle GWP, respectively. Figure 11 above, which shows that the BIPV retrofit scenarios have a different internal ratio and a lower overall carbon footprint. As a result, the building's new lower total emissions have a smaller proportion of OC.

Discussions

Interpretation of the LCA results

The BaU scenario produced total life cycle emissions of 1.73×10^7 kg CO_2e over the 20-year assessment period. The result shows two main emission hotspots. The first hotspot is operational electricity, which contributed 8.53×10^6 kg CO_2e. The second hotspot is structural material production, mainly steel and concrete. Reinforcement steel contributed 3.3×10^6 kg CO_2e, while ready-mix lightweight aggregate concrete contributed 3.0×10^6 kg CO_2e.

This result gives a different view from the common expectation for tropical buildings. In hot and humid climates, operational energy often dominates life cycle emissions because buildings need continuous cooling. This pattern appears in Malaysia and Singapore, where operational carbon made up most of the life cycle emissions [14, 16]. The present study shows a more balanced profile. Embodied carbon contributed 50.4%, while operational carbon contributed 49.6%.

Two factors explain this result. First, the assessment period is 20 years, which is shorter than the 30 to 50 year periods often used in building LCA studies. A shorter period gives more weight to upfront emissions from A1-A5 because these emissions occur before or during construction. Second, the case building uses large quantities of structural concrete and steel. These materials dominate the product stage. Together, steel and concrete accounted for most A1-A3 emissions. This means the building's carbon profile depends on both material selection and operational energy performance.

The transport stage contributed a smaller share of emissions. A4 transport reached 112,196 kg CO_2e, equal to 0.65% of total BaU emissions. Reinforcement steel dominated this stage because of its large mass. The small share of A4 does not mean transport assumptions lack importance. Rather, it shows that product-stage emission factors and operational electricity dominate the result under the model boundary. Clear reporting of transport assumptions still matters because it helps readers judge the inventory data and reproduce the assessment.

Implications for embodied and operational carbon in tropical high-rise buildings

The EC and OC split in this study adds useful evidence to the literature on tropical building decarbonization. Previous studies in tropical climates often place operational energy as the main priority. This remains relevant here because operational electricity is the largest single emission source. But the results also show that embodied carbon deserves equal attention in new high-rise residential buildings.

The result differs from older tropical building studies because the case building reflects a different context. It is a newly built high-rise residential tower in a planned capital city. Its operational energy demand is projected, while its material quantities come from as-built data. This creates a profile where upfront material emissions play a large role. The result is closer to the trend found in newer buildings in temperate contexts, where embodied emissions rise as operational performance improves [15].

This finding matters for Nusantara. If the city focuses only on operational energy reduction, it will miss a large share of building-related emissions. Low-carbon design in Nusantara should address structural material intensity, concrete mix selection, steel sourcing, prefabrication efficiency, and construction-phase emissions. Energy efficiency and renewable energy remain important, but they should sit within a whole-life carbon strategy.

BIPV Performance and Its Implications for Nusantara's NZE Target

The BIPV scenarios reduced life cycle emissions, but they did not eliminate the building's dependence on grid electricity. Scenario 1 reduced total emissions from 1.73×10^7 kg CO_2e to 1.641×10^7 kg CO_2e. This equals a reduction of 5.2%. Scenario 2 reduced total emissions to 1.549×10^7 kg CO_2e, equal to a reduction of 10.5%.

The reduction came mainly from lower B6 operational electricity emissions. Scenario 1 reduced electricity-related emissions by 0.93×10^6 kg CO_2e. Scenario 2 reduced them by 1.92×10^6 kg CO_2e. These reductions show that BIPV has a clear role in high-rise buildings where rooftop area alone limits solar generation.

The results also show the carbon trade-off from adding PV materials. BIPV increased product-stage emissions because the model added PV panels, mounting components, and related system elements. Scenario 1 increased PV-related product emissions from 33,811 kg CO_2e to 67,883 kg CO_2e. Scenario 2 increased them to 135,765 kg CO_2e. This added embodied carbon was smaller than the operational savings. The net effect stayed positive in both scenarios.

Still, the result shows the limit of BIPV as a stand-alone solution. Scenario 2 offset around 101.5 MWh/year of grid electricity, while the baseline annual electricity demand was 451.3 MWh/year. This means the larger BIPV scenario reduced electricity-related emissions by 22.5%, but most demand still came from the grid. This finding aligns with the logic in [NO_PRINTED_FORM] [41] and [NO_PRINTED_FORM] [42], where BIPV reduces operational emissions but depends on available surface area, orientation, shading, and demand profile.

For Nusantara, the implication is direct. BIPV should form one part of the building decarbonization strategy. It should be paired with passive cooling measures, efficient HVAC systems, lower-carbon materials, and a cleaner electricity supply. A previous study in eight cities also supports the need for multiple technology pathways in building carbon reduction [NO_PRINTED_FORM] [43].

Comparison With Previous Studies

The BaU emissions profile differs from several tropical building studies. A study in Malaysia reported operational carbon shares of 74.9% to 86.6% in high-rise office buildings [14]. A study in Singapore reported a 90% operational contribution in university buildings [16]. In this study, operational carbon reached 49.6%. This lower share does not contradict those studies. It reflects differences in building type, assessment period, and operational intensity.

The case building is residential, while the Malaysian and Singaporean cases were office and university buildings. Office and institutional buildings usually have higher equipment loads, longer operating schedules, and different cooling profiles. The assessment period also differs. A 20-year period gives less time for operational emissions to accumulate. This explains why embodied carbon remains high in this study.

The embodied carbon result also fits with Indonesian housing evidence. A study in Indonesia reported embodied carbon values for affordable apartments in a broad range [44]. The result in this study falls within that range, which supports the consistency of the material inventory. This comparison strengthens the credibility of the as-built quantities used in the LCA.

The BIPV results also sit within the range of previous studies, but with some differences. Scenario 1 produced a lower operational carbon reduction than the range reported in China [41]. Scenario 2 reached a similar range, with a 22.5% reduction in electricity-related emissions. The difference between scenarios shows the importance of

available PV surface area. It also confirms that façade PV needs sufficient coverage to deliver a material reduction in operational emissions.

Financial Interpretation

The financial results demonstrate that system scale significantly affects economic performance. Both scenarios were modeled using a baseline electricity consumption tariff of 0.14 AUD/kWh with an annual tariff evolution of +0.5%, a discount rate of 5.50%, and module degradation factored via the PVsyst ageing tool. Scenario 1 required a Capital Expenditure (CAPEX) of 87,688.44 AUD. The annual Operating and Maintenance (O&M) costs totaled 727.70 AUD, which included 100.00 AUD for cleaning and a 627.70 AUD replacement cost provision for inverters. This configuration resulted in a final Net Present Value (NPV) of 13,204.18 AUD and a payback period of 22.5 years. Scenario 2 required a higher CAPEX of 146,235.44 AUD. Its O&M costs were 1,361.40 AUD annually, comprising 100.00 AUD for cleaning and a 1,261.40 AUD replacement cost provision for inverters. Despite the higher initial investment and operational expenses, Scenario 2 achieved a superior NPV of 19,583.97 AUD and a shorter payback period of 16.3 years.

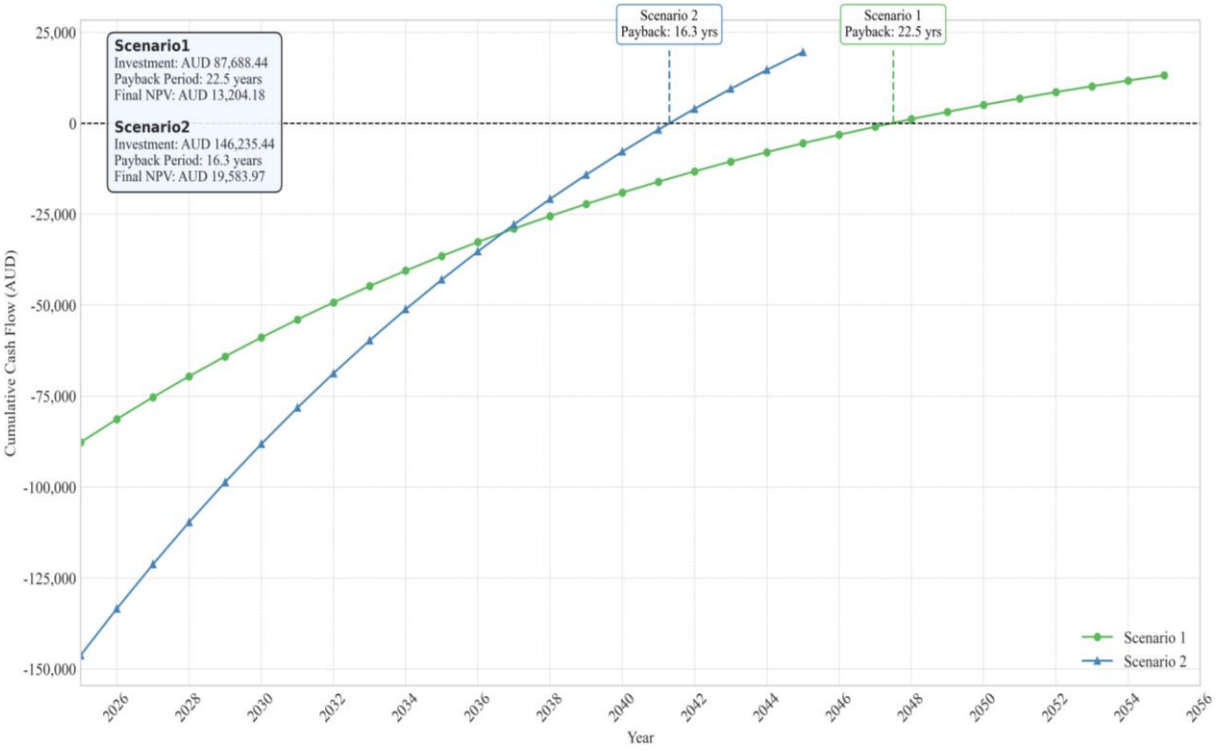


Figure 12. Financial analysis of the BIPV systems

Scenario 2 performed better economically because it generated more electricity, offsetting its higher costs and delivering higher carbon savings. Crucially, Scenario 1 is not financially viable because its 22.5-year payback period exceeds the standard 20-year assessment period utilized for Scenario 2. Overall payback periods remain longer than some international BIPV cases, for example, the Kunming case [45]. A key reason is the absence of a feed-in tariff in this study; the financial model provides a conservative estimate by counting savings from avoided grid electricity only, without factoring in revenue from exported electricity. These financial results highlight the relevance of policy mechanisms. Without tariff design, capital incentives, or procurement rules, building owners may delay investment or opt for smaller systems. In contrast, stronger policy support would make larger, more optimal installations like Scenario 2 highly attractive.

Uncertainty and Sensitivity of Results

A GSA was done using the variance-based Sobol method. The analysis was carried out through a Monte Carlo simulation, in which the GWP of each of the twelve lifecycle phases was treated as an uncertain input parameter. The simulation produced thousands of model outcomes, which were then examined to calculate the Sobol indices: the first-order index (S_1) measures the direct effect of a single parameter on output variance, while the total-order index (S_T) captures a parameter's overall contribution, including its direct effect and the effects from its interactions with other parameters [37].

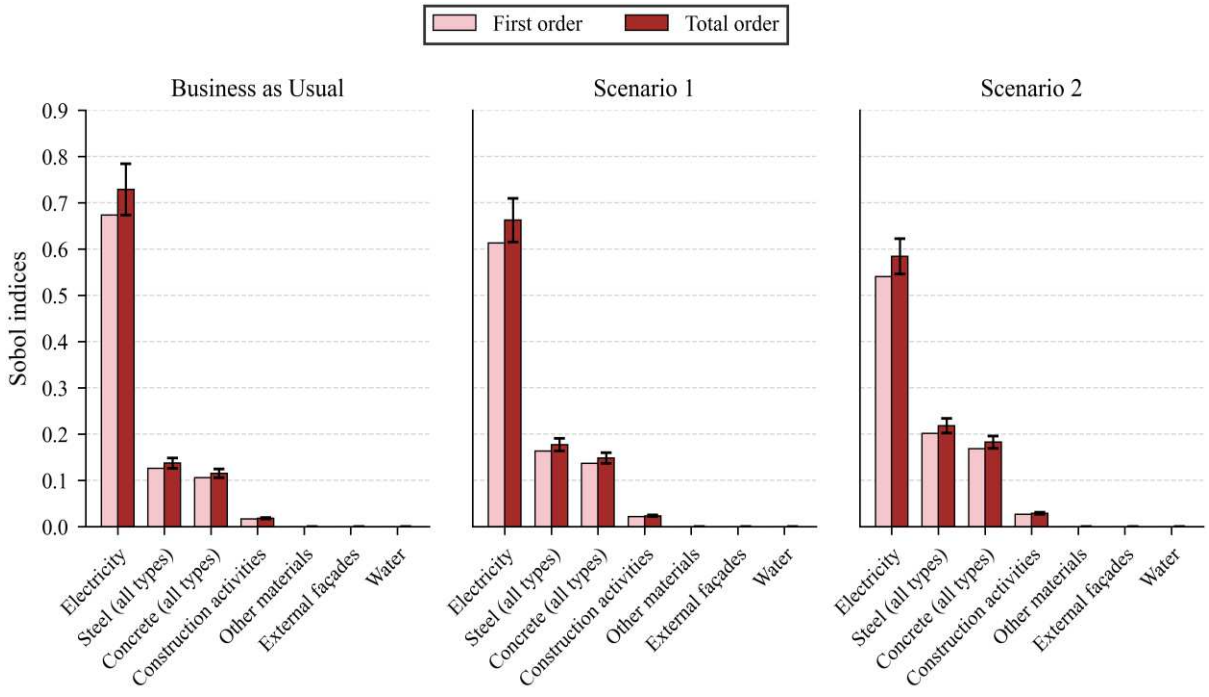


Figure 13. Global sensitivity analysis with Monte Carlo simulation for the BaU, Scenario 1, and Scenario 2. This chart ranks lifecycle phases by their contribution to the total GWP uncertainty. A longer bar indicates a more sensitive parameter

The analysis results, shown in Figure X, clearly rank the lifecycle phases based on their impact on the overall uncertainty of the total GWP. The most sensitive parameter in all scenarios is clearly operational electricity, which has the highest total-order index (ST). This means that uncertainty in the building's energy use is the main cause of uncertainty in its total carbon footprint. The next most important parameters are the embodied carbon of structural materials (i.e., steel, concrete), and construction activities. On the other hand, several phases, including other materials, external facades, and operational water, show Sobol indices close to zero. This indicates that their uncertainties have little effect on the variance of the final LCA result [37, 38]. The degree of sensitivity differs in three scenarios, as the composition of the input parameters changes.

Conclusions

This study delivers a comprehensive life cycle carbon assessment for high-rise residential buildings in Nusantara, providing empirical evidence to guide the city's 2045 NZE mandate. The evaluation demonstrates a critical paradigm shift in tropical building emissions: over a targeted 20-year assessment period, EC accounts for 50.4% of the total life-cycle footprint, marginally exceeding OC at 49.6%. This confirms that as operational efficiencies improve, the manufacturing of structural materials, specifically concrete and steel, constitutes an immediate and dominant carbon hotspot. The integration of BIPV presents a financially viable decarbonization strategy, though system scale dictates its overall success. The modeled 93.0 kWp BIPV system (Scenario 2) achieved a 10.5% reduction in total life-cycle carbon emissions with a payback period of 16.3 years and a NPV of AUD 19,583.97. Conversely, the smaller 46.5 kWp system (Scenario 1) yielded a 22.5-year payback, rendering it financially non-viable within the 20-year analytical boundary. Furthermore, the variance-based GSA confirms that uncertainties in grid electricity and structural material manufacturing strictly dictate the overall emission variance. To achieve substantial decarbonization, policymakers must enforce holistic building codes that simultaneously cap embodied material intensity and incentivize on-site renewable energy through capital subsidies, net-metering, or feed-in tariffs. Future research should focus on developing a localized Indonesian LCI database to reduce modelling uncertainties and evaluating alternative low-carbon structural systems, such as engineered timber or high-volume fly-ash concrete, to further mitigate embodied emissions.

Data availability statement

Data that support the findings of this study are available upon reasonable request from the authors.

Acknowledgement

This work was conducted within the Department of Infrastructure Engineering, The University of Melbourne, Australia, as a master's research project of the first author. This work is supported by the Indonesian Government and the Australian Department of Foreign Affairs and Trade through LPDP – AAS Scholarship (funding no: 0033560/GRE/M/AAS-2024).

Author contributions statement

Rudi Chandra Adinugraha: Writing – original draft, Visualization, Validation, Methodology, Investigation, Formal analysis, Data curation, Conceptualization. **Mohamed Ali Berawi**: Resources, Writing – review & editing. **Titi Sari Nurul Rachmawati**: Validation, Writing – review & editing. **Behzad Rismanchi**: Writing – review & editing, Validation, Supervision, Project administration, Conceptualization.

Declaration of interests

The authors declare that they have no known competing financial interests or personal relationships that could have appeared to influence the work reported in this paper.

Ethics, Consent to Participate, and Consent to Public declarations

Not applicable.

References

1. Nejat P, Jomehzadeh F, Taheri MM, et al (2015) A global review of energy consumption, CO_2 emissions and policy in the residential sector (with an overview of the top ten CO_2 emitting countries). Renewable and Sustainable Energy Reviews 43:843–862. https://doi.org/10.1016/j.rser.2014.11.066
2. Lai F, Zhou J, Lu L, et al (2023) Green building technologies in Southeast Asia: A review. Sustainable Energy Technologies and Assessments 55:102946. https://doi.org/10.1016/j.seta.2022.102946
3. Dervishaj A, Gudmundsson K (2024) From LCA to circular design: A comparative study of digital tools for the built environment. Resour Conserv Recycl 200: https://doi.org/10.1016/j.resconrec.2023.107291
4. Sachdeva S, Hsu A, French I, Lim E (2022) A computational approach to analyzing climate strategies of cities pledging net zero. npj Urban Sustainability 2: https://doi.org/10.1038/s42949-022-00065-x
5. Black J, Nakanishi H (2024) Towards Net-Zero Emissions from Urban Transport: Ex Post Policy Evaluation in Canberra, the Australian Capital Territory. Sustainability 16:8656. https://doi.org/10.3390/su16198656
6. Wijayanto T, Hakam DF, Kemala PN (2025) Vision for Indonesia's 2050 power generation: Scenarios of hydrogen integration, nuclear energy prospects, and coal phase-out impact. Sustainable Futures 9: https://doi.org/10.1016/j.sftr.2025.100438
7. The Government of Indonesia (2022) Law No. 3 of 2022 concerning the National Capital of Indonesia. Indonesia
8. Keyhani M, Bahadori-Jahromi A, Fu C, et al (2024) Whole-Life Embodied Carbon Reduction Strategies in UK Buildings: A Comprehensive Analysis. Energy Sci Eng 12:5370–5384. https://doi.org/10.1002/ese3.1958
9. Liang Y, Li C, Liu Z, et al (2023) Decarbonization potentials of the embodied energy use and operational process in buildings: A review from the life-cycle perspective. Heliyon 9:e20190. https://doi.org/10.1016/j.heliyon.2023.e20190
10. Nwodo MN, Anumba CJ (2019) A review of life cycle assessment of buildings using a systematic approach. Build Environ 162:106290. https://doi.org/10.1016/j.buildenv.2019.106290
11. Liu Z, Zhang Y, Yuan X, et al (2021) A comprehensive study of feasibility and applicability of building integrated photovoltaic (BIPV) systems in regions with high solar irradiance. J Clean Prod 307:127240. https://doi.org/10.1016/j.jclepro.2021.127240
12. Lützkendorf T, Balouktsi M (2022) Embodied carbon emissions in buildings: explanations, interpretations, recommendations. Buildings and Cities 3:964–973. https://doi.org/10.5334/bc.257
13. Ma L, Azari R, Elnimeiri M (2024) A Building Information Modeling-Based Life Cycle Assessment of the Embodied Carbon and Environmental Impacts of High-Rise Building Structures: A Case Study. Sustainability (Switzerland) 16: https://doi.org/10.3390/su16020569
14. Mulya KS, Ng WL, Biró K, et al (2024) Decarbonizing the high-rise office building: A life cycle carbon assessment to green building rating systems in a tropical country. Build Environ 255: https://doi.org/10.1016/j.buildenv.2024.111437

15. Li S, Foliente G, Seo S, et al (2021) Multi-scale life cycle energy analysis of residential buildings in Victoria, Australia – A typology perspective. Build Environ 195: https://doi.org/10.1016/j.buildenv.2021.107723

16. Chang CC, Shi W, Mehta P, Dauwels J (2019) Life cycle energy assessment of university buildings in tropical climate. J Clean Prod 239: https://doi.org/10.1016/j.jclepro.2019.117930

17. Alotaibi BS, Khan SA, Abuhussain MA, et al (2022) Life Cycle Assessment of Embodied Carbon and Strategies for Decarbonization of a High-Rise Residential Building. Buildings 12: https://doi.org/10.3390/buildings12081203

18. Santos R, Costa AA, Silvestre JD, et al (2020) BIM-based life cycle assessment and life cycle costing of an office building in Western Europe. Build Environ 169: https://doi.org/10.1016/j.buildenv.2019.106568

19. Rydlewski J, Rajabi Z, Tariq MAUR, et al (2022) Identification of Embodied Environmental Attributes of Construction in Metropolitan and Growth Region of Melbourne, Australia to Support Urban Planning. Sustainability 14:8401. https://doi.org/10.3390/su14148401

20. Fenner AE, Kibert CJ, Li J, et al (2020) Embodied, operation, and commuting emissions: A case study comparing the carbon hotspots of an educational building. J Clean Prod 268: https://doi.org/10.1016/j.jclepro.2020.122081

21. Luo XJ (2023) An integrated passive and active retrofitting approach toward minimum whole-life carbon footprint. Energy Build 295: https://doi.org/10.1016/j.enbuild.2023.113337

22. Bahramian M, Yetilmezsoy K (2020) Life cycle assessment of the building industry: An overview of two decades of research (1995–2018). Energy Build 219:109917. https://doi.org/10.1016/j.enbuild.2020.109917

23. Karunaratne S, Dharmarathna D (2022) A review of comprehensiveness, user-friendliness, and contribution for sustainable design of whole building environmental life cycle assessment software tools. Build Environ 212:108784. https://doi.org/10.1016/j.buildenv.2022.108784

24. Fnais A, Rezgui Y, Petri I, et al (2022) The application of life cycle assessment in buildings: challenges, and directions for future research. Int J Life Cycle Assess 27:627–654. https://doi.org/10.1007/s11367-022-02058-5

25. Cavalliere C, Dell'Osso GR, Pierucci A, Iannone F (2018) Life cycle assessment data structure for building information modelling. J Clean Prod 199:193–204. https://doi.org/10.1016/j.jclepro.2018.07.149

26. Grant A, Ries R, Kibert C (2014) Life cycle assessment and service life prediction: A case study of building envelope materials. J Ind Ecol 18:187–200. https://doi.org/10.1111/jiec.12089

27. Khan SA, Alam T, Khan MS, et al (2022) Life Cycle Assessment of Embodied Carbon in Buildings: Background, Approaches and Advancements. Buildings 12:1944. https://doi.org/10.3390/buildings12111944

28. Bisinella V, Conradsen K, Christensen TH, Astrup TF (2016) A global approach for sparse representation of uncertainty in Life Cycle Assessments of waste management systems. International Journal of Life Cycle Assessment 21:378–394. https://doi.org/10.1007/s11367-015-1014-4

29. Zhang T, Wang M, Yang H (2018) A Review of the Energy Performance and Life-Cycle Assessment of Building-Integrated Photovoltaic (BIPV) Systems. Energies (Basel) 11:3157. https://doi.org/10.3390/en11113157

30. Yu G, Yang H, Yan Z, Kyeredey Ansah M (2021) A review of designs and performance of façade-based building integrated photovoltaic-thermal (BIPVT) systems. Appl Therm Eng 182: https://doi.org/10.1016/j.applthermaleng.2020.116081

31. Martín-Chivelet N, Gutiérrez JC, Alonso-Abella M, et al (2018) Building retrofit with photovoltaics: Construction and performance of a BIPV ventilated façade. Energies (Basel) 11: https://doi.org/10.3390/en11071719

32. Pham MH, Phap VM, Trung NN, et al (2022) A Study on the Impact of Various Meteorological Data on the Design Performance of Rooftop Solar Power Projects in Vietnam: A Case Study of Electric Power University. Energies (Basel) 15: https://doi.org/10.3390/en15197149

33. Habte A, Sengupta M, Lopez A (2017) Evaluation of the National Solar Radiation Database (NSRDB Version 2): 1998-2015

34. Tripathy M, Joshi H, Panda SK (2017) Energy payback time and life-cycle cost analysis of building integrated photovoltaic thermal system influenced by adverse effect of shadow. Appl Energy 208:376–389. https://doi.org/10.1016/j.apenergy.2017.10.025

35. Fauzi RT, Lavoie P, Tanguy A, Amor B (2021) Life cycle assessment and life cycle costing of multistorey building: Attributional and consequential perspectives. Build Environ 197: https://doi.org/10.1016/j.buildenv.2021.107836

36. Pangestu M, Armstrong S (2025) Is This Time Different? Indonesia's Response to Uncertainty. Bull Indones Econ Stud 61:297–332. https://doi.org/10.1080/00074918.2025.2588819

37. Kim A, Mutel C, Hellweg S (2025) Global sensitivity analysis of correlated uncertainties in life cycle assessment. J Ind Ecol. https://doi.org/10.1111/jiec.70036

38. Wei W, Larrey-Lassalle P, Faure T, et al (2015) How to conduct a proper sensitivity analysis in life cycle assessment: Taking into account correlations within LCI data and interactions within the LCA calculation model. Environ Sci Technol 49:377–385. https://doi.org/10.1021/es502128k

39. Yang RJ, Zhao Y, Jayakumari SDS, et al (2024) Digitalising BIPV energy simulation: A cross tool investigation. Energy Build 318: https://doi.org/10.1016/j.enbuild.2024.114484

40. Goel S, Sharma R (2021) Analysis of measured and simulated performance of a grid-connected PV system in eastern India. Environ Dev Sustain 23:451–476. https://doi.org/10.1007/s10668-020-00591-7

41. Pan D, Yu X, Zhou Y (2023) Cradle-to-grave lifecycle carbon footprint analysis and frontier decarbonization pathways of district buildings in subtropical Guangzhou, China. J Clean Prod 416: https://doi.org/10.1016/j.jclepro.2023.137921

42. Shono K, Yamaguchi Y, Perwez U, et al (2023) Large-scale building-integrated photovoltaics installation on building façades: Hourly resolution analysis using commercial building stock in Tokyo, Japan. Solar Energy 253:137–153. https://doi.org/10.1016/j.solener.2023.02.025

43. Ang YQ, Berzolla ZM, Letellier-Duchesne S, Reinhart CF (2023) Carbon reduction technology pathways for existing buildings in eight cities. Nat Commun 14: https://doi.org/10.1038/s41467-023-37131-6

44. Agustiningtyas RS, Takaguchi H, Prasetya AB, Kubota T (2023) Embodied energy and carbon assessment of existing affordable apartments in Indonesia. J Asian Arch and Build Eng. https://doi.org/10.1080/13467581.2023.2278481

45. Wang Y, Li M, Hassanien RHE, et al (2018) Grid-connected semitransparent building-integrated photovoltaic system: The comprehensive case study of the 120kWp plant in Kunming, China. Intl J of Photoenergy 2018: https://doi.org/10.1155/2018/6510487